



Depósito de Investigación de la Universidad de Sevilla

<https://idus.us.es/>

This is an Accepted Manuscript of an article published by Elsevier in
Composites Science and Technology
Vol. 124, on March 2016, available at:

<https://doi.org/10.1016/j.compscitech.2016.01.003>

Copyright 2016 Elsevier. En idUS Licencia Creative Commons CC BY-NC-ND

Tensile and shear strength of bimaterial interfaces within composite materials

Alberto Barroso¹, Bernd Lauke², Vladislav Mantič¹, Federico París¹

¹ Elasticity and Strength of Materials Group, School of Engineering, University of Seville, Camino de los Descubrimientos s/n, 41092, Seville, Spain

² Leibniz-Institut für Polymerforschung Dresden e. V., Hohe Strasse 6, 01069 Dresden, Germany

Corresponding author:

Alberto Barroso

Elasticity and Strength of Materials Group

School of Engineering, University of Seville, Camino de los Descubrimientos s/n
41092 Sevilla

Spain

Email: abc@us.es

Tensile and shear strength of bimaterial interfaces within composite materials

Abstract: The determination of the tensile and shear strengths of homogeneous materials can be easily performed by standard tensile and shear (e.g. Iosipescu) tests. Nevertheless, when the determination of these strengths involves a bimaterial interface, the standard samples present bimaterial corner configurations at their free-edges which generate singular stress fields. In the presence of these singular stress fields, the tensile and shear stress distributions are strongly non-uniform at these edges, where failure initiates and propagates along the bimaterial interface. The apparent strength obtained from these tests is not representative of the regularized strength of the bimaterial interface. To eliminate the stress singularities, a small notch is made on one of the materials along the interface perimeter, in this study. This idea, originally proposed by Lauke and Barroso (Compos. Interface, 18:661-669, 2011) for ascertaining tensile strength, is now adapted to ascertain shear strength, using a modified geometry of the Iosipescu sample, and it has also been generalized to configurations involving composite materials. Both proposals, for the tensile and shear tests, are performed using the bimaterial configuration of a composite and an adhesive; a bimaterial interface which typically appears in adhesive joints with composites. The local notch geometry is defined using semi-analytical tools developed by the authors and numerically verified by Finite Element models. The modified bimaterial geometries, tested under tension, demonstrated a higher tensile strength. However, the modified bimaterial geometries tested in shear did not show any clear influence over the failure load with or without the notch in the particular bimaterial configuration tested in this study.

Keywords: Adhesive joints, Interfacial strength, Stress singularities, Iosipescu test, Joining.

1 Introduction

Failure prediction for structural components containing bimaterial interfaces may require knowledge of the normal and shear strengths of the interface. Failure criteria typically compare some combination of stresses/strains/displacements with their corresponding critical values. This study is mainly motivated by the need to ascertain some of these critical values (in particular the tensile and shear strengths values), for potential failure paths in adhesive joints which involve bimaterial interfaces (Figure 1), for the purposes of predicting failure initiation. From the three potential failure paths shown in Figure 1 (which start at the critical corner point, where failure typically begins [2]), path “a” involves only one material (adhesive), whose tensile and shear strengths can easily be determined by standard test procedures. However, paths “b” and “c” involve bimaterial interfaces with different fibre orientations, which might have different strengths. Along failure path “b”, the fibre orientation is perpendicular to the interface plane, whereas along path “c”, the fibre orientation is parallel to the interface plane.

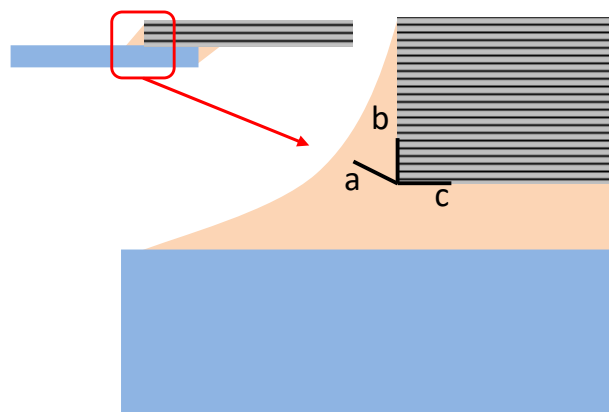


Figure 1. Failure paths initiated at the critical corner point of an adhesive joint.

The problem arises when trying to determine the strengths (e.g., the tensile strengths) associated with these alternative failure paths. Figure 2 shows the natural choices for the

bimaterial specimen configurations for determining the tensile strength. Figures 2a, b and c correspond to failure paths “a”, “b” and “c” respectively. Figure 2d will be discussed later. Nevertheless, samples in Figures 2b and c (butt samples with a flat bimaterial interface) have, at the free edges of the samples, bimaterial corner configurations which give rise to stress singularities due to the material properties mismatch. The tensile stresses are non-uniform along the interface. Thus, the tensile strength at the instant of failure (calculated as the failure load divided by the cross-sectional area of the sample) is not representative of the nominal adhesion strength, under tension, of the interface. The transverse section of these butt samples is of a rectangular shape whose width, represented in Figure 2, is usually much larger than its thickness.

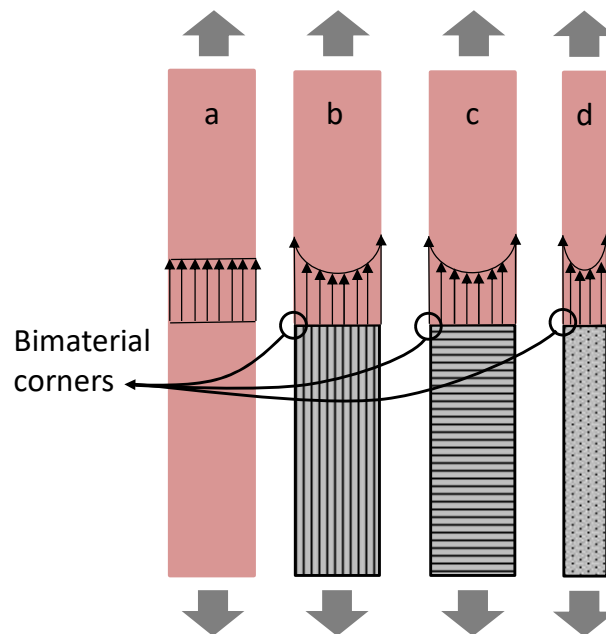


Figure 2. Reference configurations for determining the adhesion strength: a) adhesive bulk configuration, b) bimaterial configuration with the fibre perpendicular to the interface, c) bimaterial configuration with the fibre parallel to the interface, d) bimaterial configuration with the fibre parallel to the interface and perpendicular to the sample plane.

Lauke and co-workers [3-6] proposed bimaterial samples with a curved interface to avoid the stress singularities. This idea was also used by Wetherhold and Dargush [7] and Chowdhuri and Xia [8] to determine the adhesive strength between epoxy-aluminum joints, and also by Wu [9]. Lauke and Barroso [1] proposed a simpler modification of the butt-test with a flat interface, including a little notch at the free edge, which generates a particular local bimaterial corner configuration and avoids the singular stress field. Although both proposals require the calculation of the corner angles where the singularities vanish, the second option is easier to manufacture. In any case, there are no proposals, to the best knowledge of the authors, for the shear strength determination of bimaterial interfaces. The use of notches to eliminate the stress singularities in the Iosipescu test, with a bimaterial configuration, is the main contribution of the present work. Moreover, the presence of composite materials in the new tensile and shear configurations make the calculations of the stress singularities not straightforward, due to the non-isotropic behaviour of the composite material. In the present work this has been solved using the tool developed by the authors to calculate the stress singularities in multimaterial anisotropic corners [12,13], which also represents a difference with previously mentioned works.

The idea of using notches to relieve stress singularities is not new (e.g. Bijak-Zochowski et al. [10]) using photoelasticity images. An alternative idea, changing the bimaterial geometry configuration locally, but not using notches, was proposed by Wang and Xu [11] for two isotropic materials.

In the present study, the determination of the tensile and shear strengths of bimaterial interfaces similar to the configurations “b” and “c” in Figures 1 and 2 will be considered. The proposal made by Lauke and Barroso [1] will be used in order to

determine the tensile strength. In order to determine the shear strength, a new proposal, based on a modification of the Iosipescu geometry, will be defined in which the shear stress singularities at the free edges are removed. To achieve this objective, analytical calculations for the local corner configurations will be performed in order to determine the correct angle at which the stress singularity vanishes. Numerical models will be developed to check the uniformity of the shear stress distribution along the flat interface in the shear test. The confirmation of the elimination of the stress singularity in the tensile test sample was carried out beforehand in [1] for a bimaterial (both isotropic) configuration. Finally, fabrication of the samples and tests will be carried out in tension and shear for the bimaterial configurations “b” and “c” in Figure 2.

2 Definition of the modified tensile and shear test samples

At a bimaterial corner, assuming linear elasticity and anisotropic behaviour of materials, the asymptotic stress field can be singular due to the mismatch in the material properties. Using a polar coordinate reference system with the centre at the corner tip, the stress state is defined by the asymptotic series expansion

$$\sigma_{ij}(r, \theta) \approx \sum_{k=1}^n K_k \cdot r^{-\lambda_k} f_{ij}^{(k)}(\theta) \quad (1)$$

Where K_k are the Generalized Stress Intensity Factors, λ_k are the stress singularity orders, and $f_{ij}^{(k)}(\theta)$ are the characteristic angular shape functions associated to this corner. Both λ_k and $f_{ij}^{(k)}(\theta)$ can be computed semi-analytically following [12,13], where all manipulations are analytical except for the final calculation of the roots of a characteristic equation, which are computed numerically.

For the two bimaterial configurations under analysis (with the fibre orientation perpendicular and parallel to the interface) and for all the corner angles considered (see Figures 2 and 3), there is only one singular term ($0 < \lambda < 1$) which dominates the stress field as $r \rightarrow 0$ because the associate stresses become unbounded. This fact has been verified by using the Argument's Principle (e.g. [13,14]), which is an excellent tool for identifying the number of roots of a holomorphic function in a particular region of the complex plane. This observation can be explained by the small corner angle (occupied by the bimaterial configuration), considered equal to 180° in Figure 2 (and less than 180° in Figure 3) which, from a geometrical point of view, does not generate a re-entrant corner configuration. Recall that in homogeneous materials there are no stress singularities at all for such corner angle values (this can be easily shown by applying the Cauchy Lemma at both traction free corner faces). Thus, the stress singularity order computed is essentially caused by the material mismatch as already mentioned above. Due to the material symmetries, the solution for the generalized plane strain problems for the present corner configurations can be decoupled into the in-plane and anti-plane solutions [15], the singular stress state corresponding to the in-plane solution. It has been checked using procedures developed in [12,13,16] that there are no singularities in the anti-plane solutions for the present corner problems for the corner angles less than, or equal to 180° .

The stress singularity order λ defines the singular character of the stress field and its value depends on the local configuration of the corner (which includes the elastic properties of the materials, local geometry and local boundary conditions). Thus, for the aim of the present study, it is only necessary to find the local geometry which makes λ zero or negative, for the stresses to be regular (non-singular) at the corner tip. The elastic properties of the carbon fibre reinforced plastic (CFRP, AS4-8552) and the

epoxy adhesive (FM-73M0.6) are: $E_{11}=141.3$ GPa, $E_{22}=E_{33}=9.58$ GPa, $G_{12}=G_{13}=5.0$ GPa, $G_{23}=3.5$ GPa, $\nu_{12}=\nu_{13}=0.3$, $\nu_{23}=0.32$ (where subindex “1” defines the fibre direction) and $E=3.0$ GPa, $\nu=0.35$, respectively. The calculations of the stress singularity orders were performed for the two basic bimaterial configurations under investigation and are summarized in Figure 3. The results shown in Figure 3 were obtained by modifying the corner angle of the adhesive at the interface, because it is much easier to do the machining on the epoxy side rather than on the CFRP side.

The results in Figure 3 show that, for the configurations associated with the failure path “b” (see Figure 1), with the fibre perpendicular to the interface, the stresses are not singular for a corner angle of the epoxy adhesive (the angle α measured from the interface), for $\alpha \delta 65^\circ$. For the configuration associated with the failure path “c”, with the fibre parallel to the interface, the singularity disappears for a corner angle of the adhesive side, for $\alpha \delta 75^\circ$. For the sake of simplicity, the selected angle for both configurations is 65° , which essentially eliminates the singularity in both bimaterial configurations.

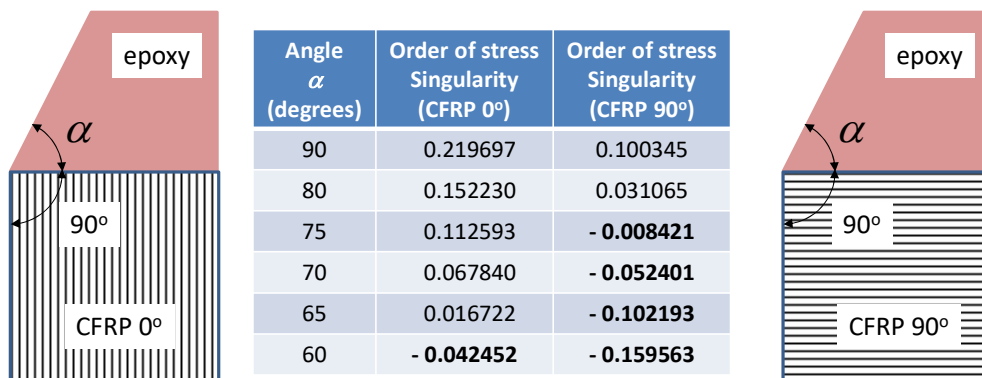


Figure 3. The order of stress singularity λ for the two bimaterial configurations in generalized plane strain.

The real 3D tensile test sample in the 0° configuration (Figure 2b) has the entire

interface perimeter with the same bimaterial corner configuration, (the fibres being perpendicular to the interface plane as shown in Figure 2b), with the actual local corner configuration being visible in Figure 3 (left configuration).

In contrast, in the 90° configuration (Figure 2c), the longest side (width) of the transversal section has the fibres parallel to this side, while the shortest side (thickness) of the transversal section (which is not visible in Figure 2c but it is schematically shown in Figure 2d), has the fibres parallel to the interface plane (as in the longest side), but perpendicular to this shortest side.

It is therefore understood that the two situations, represented as corresponding to independent samples in Figure 2 (c and d), appear for the same sample in the 90° configuration, at the two different sides.

The order of stress singularity has also been calculated for the fibre orientation corresponding to the configuration shown in Figure 2d, and, somewhat surprisingly, is exactly equal to that of case 2b. Thus, the corner angle $\alpha \delta 65^\circ$ fulfils the condition of eliminating the stress singularities for all the material configurations considered.

Figure 4 and Figure 5, respectively, show the modifications carried out on the tensile sample (Figure 4) and shear, so-called Iosipescu, sample (Figure 5). As will be explained in detail below, the notch in the tensile sample is made all around the interface perimeter, whereas the notch in the shear sample is only made along the short sides of the interface section, in view of the shear load direction. This is because, as mentioned above, there is no anti-plane stress singularity for the bimaterial corner angle of 180°. Thus, no anti-plane stress singularity can be activated along the long interface side (width) in this shear test.

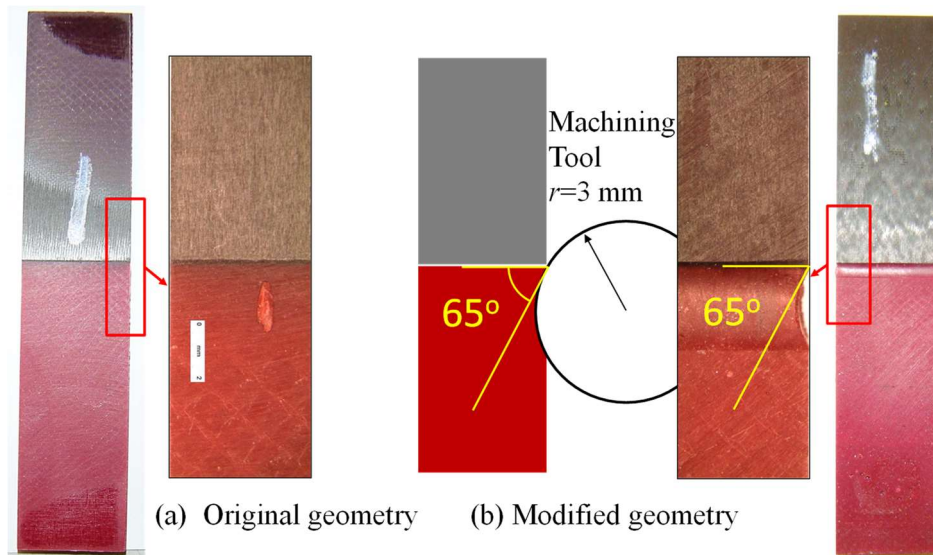


Figure 4. Machining of the tensile samples to eliminate the stress singularity.

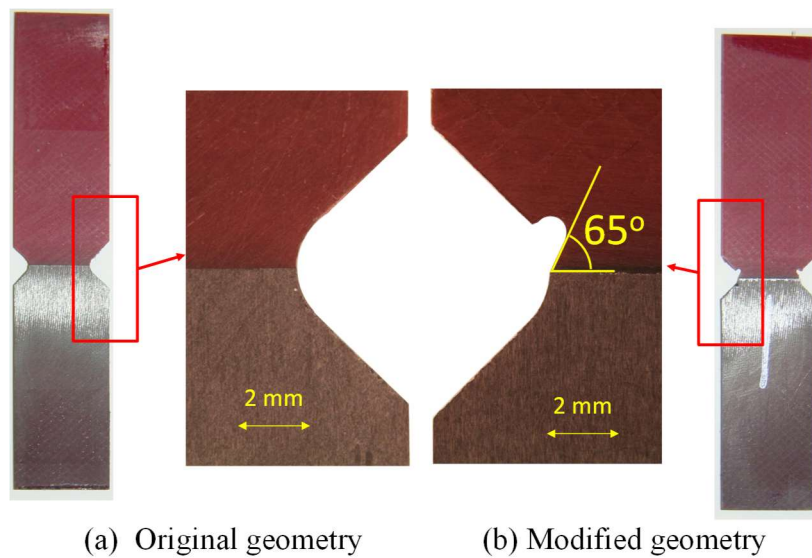


Figure 5. Machining of the shear (Iosipescu) samples to eliminate the stress singularity.

In the tensile notched butt-test samples, the local machining of the coupons was carried out all around the interface perimeter using a tool with $r=3$ mm (Figure 4). The machining was delicate, as the depth required to achieve the desired 65° configuration is only 0.281 mm. This modification, as mentioned previously, is similar to that proposed

in [1].

In the Iosipescu samples, the local machining was only performed along the shortest free edges of the interface (Figure 5). Recall that the long, non-machined side of the interface section in the Iosipescu test is subjected to a kind of tearing mode (anti-plane mode) along this line. Nevertheless, as mentioned above, the calculations carried out to determine the order of stress singularity revealed that there is no stress singularity associated with this mode. Recall that in all the configurations of bimaterial interfaces analysed in Figure 2, the in-plane behaviour is not coupled with the antiplane behaviour due to the presence of the symmetry planes of the bimaterial configuration.

All samples were inspected using a microscope at ($\times 50$). No damage was observed due to the machining process and the measured values of the angle produced by the machining were quite accurate ($65^\circ \pm 2^\circ$).

A Finite Element Method (FEM) model was developed in order to check, from a numerical point of view, the suppression of the stress singularity at the free edge and the degree of uniformity of the shear stresses along the interface in the modified shear sample. Loading in the FEM model was applied following the indications in [17]. In the model, an appropriate mesh refinement towards the corner tip was used, with an element size of 10^{-3} mm adjacent to the free edge.

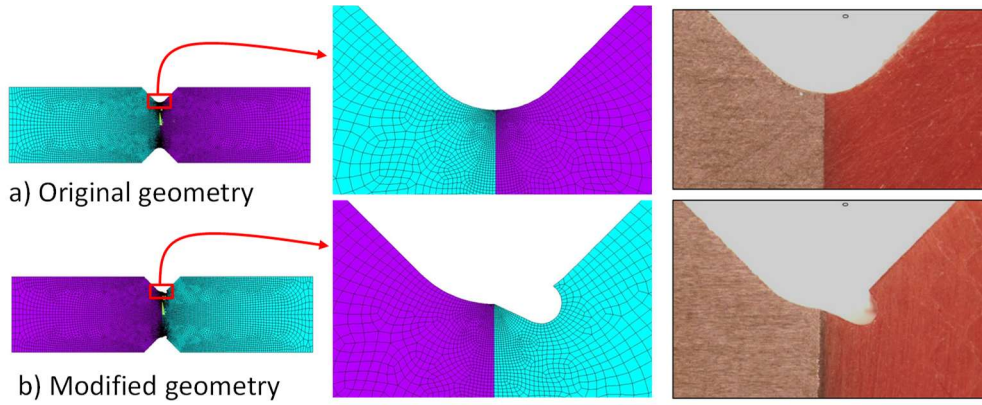


Figure 6. Finite element model of a) the original, and b) the modified configurations, and real pictures of the samples.

Figure 7 shows the shear stress distribution along the interface of the planar model, for the bimaterial sample with the fibre direction perpendicular to the interface. Although the real test sample geometry would more likely behave in a plane stress state, in Figure 7, the shear stress distribution has also been calculated for the plane strain state.

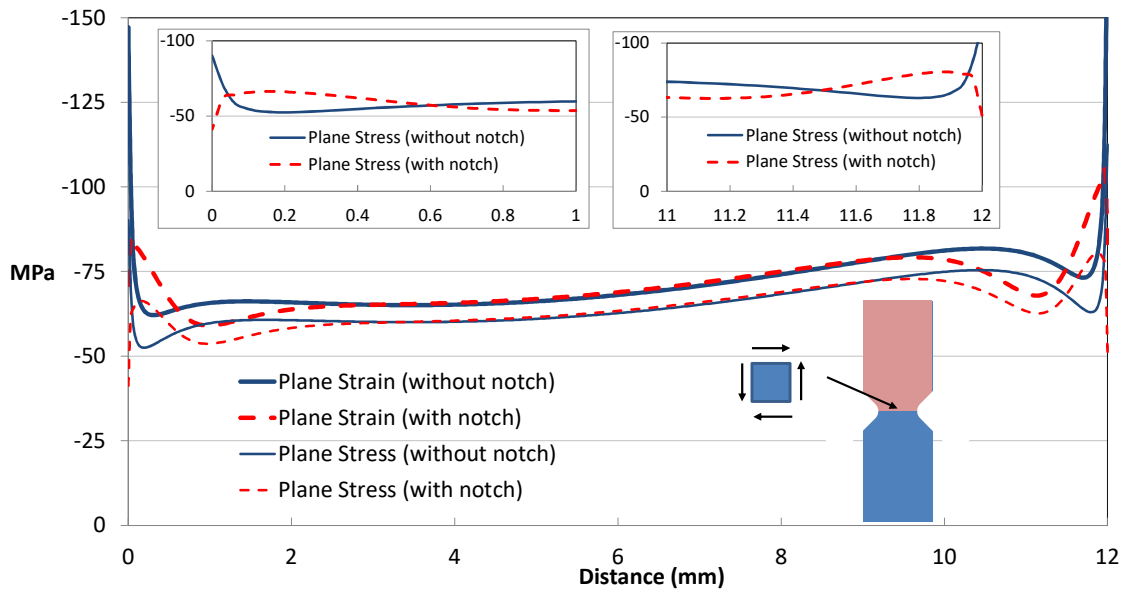


Figure 7. Finite element results for the shear stresses along the interface, for the original and modified configurations of the Iosipescu sample (fibre orientation in the composite lamina is perpendicular to the interface).

It can be clearly seen in Figure 7 that, as predicted, the notch at the free edges

eliminates the stress singularities. Specifically, in the geometry without the notch, the shear stresses become unbounded as far as the mesh is refined (assuming a linear elastic analysis), whereas in the case of the notched geometry, the shear stresses tend to vanish with progressive mesh refinements. However, firstly due to the lack of symmetry of the bimaterial sample and, secondly, to the presence of the free edges and the notch itself, the shear stress distribution along the interface is not absolutely constant, but quite uniform, which means that a representative shear strength is expected to be determined at the instant of failure, as happens when the Iosipescu test is used to determine stiffness/strength properties for homogeneous composite specimens.

The corresponding results for the tensile samples are shown in Figure 8, in which, the composite material has the fibre direction perpendicular to the interface. Both, plane strain and plane stress conditions have been computed for configurations with and without notch. In Figure 8, the normal stress at the interface (σ_{xx}) divided by the remote nominal tensile stress (σ_0) is represented along the interface (only half of the model has been calculated due to the symmetry). It can be clearly seen that the configurations without notch have stress singularities at the free edge, while configurations with the notch do not have the stress singularity and give rise to stress distributions which are mainly constant along the interface.

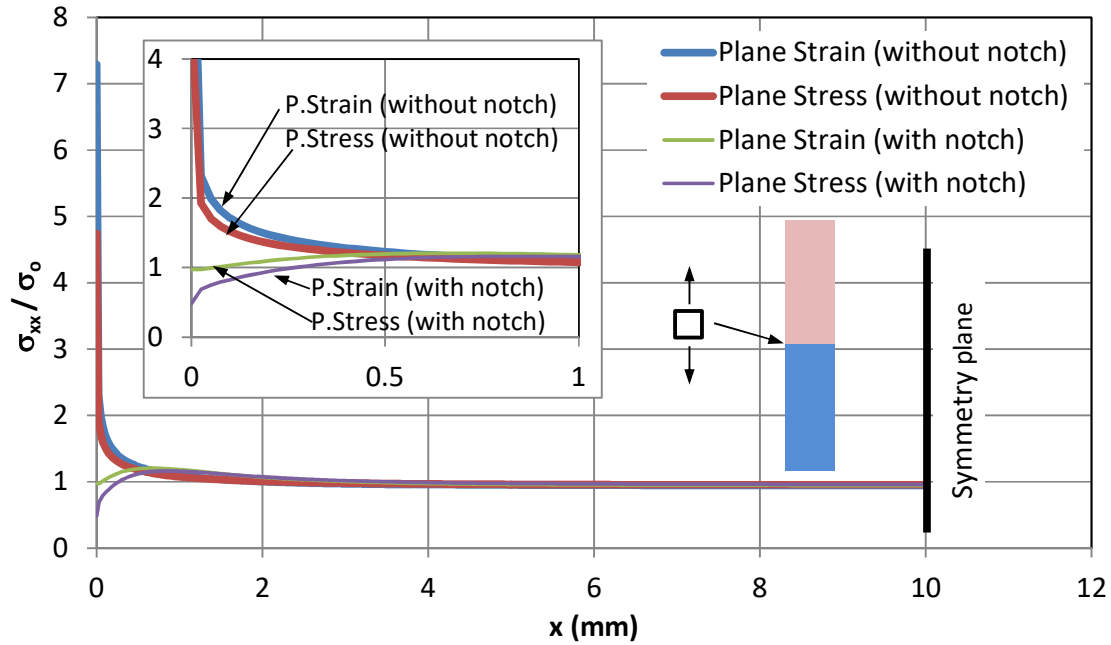


Figure 8. Finite element results for the normal stresses along the interface, for the original and modified configurations of the tensile sample (fibre orientation in the composite lamina is perpendicular to the interface).

3 Test results

3.1 Manufacturing of the samples

To prepare the samples, already cured composite laminates were used. Adhesive layers were laminated adjacent to the composite laminates (Figure 9a), using a vacuum bag for each five adhesive laminas to help the compactation process. Then, the adhesive laminate was cured according to the curing cycle supplied by the manufacturer (90 minutes, 120°C) (Figure 9b). The adhesive was laminated to get a little larger thickness than that of the cured composite laminate (Figure 9c), to allow a final thickness control in the machining process (Figure 9d). Finally, the samples were polished, before testing, to eliminate surface irregularities.

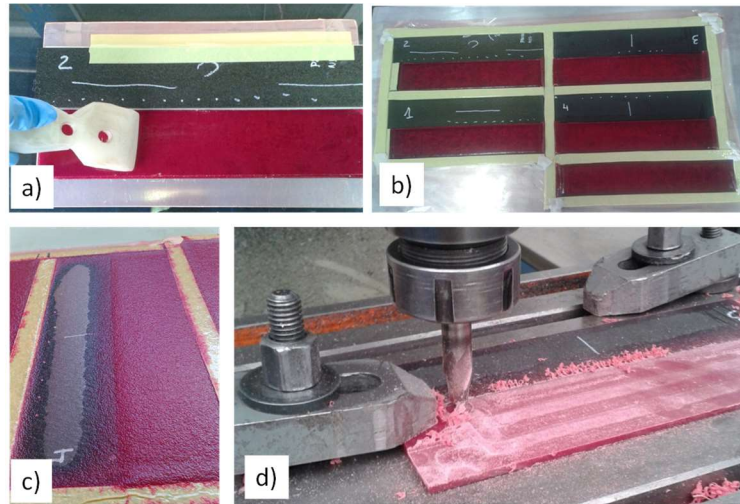


Figure 9. a) Lamination of the adhesive, b) samples ready to autoclave curing, c) samples after curing, d) machining of samples to get constant thickness.

3.2 Tensile tests

Tensile samples were tested in a universal testing machine under tension at a cross-head speed of 2 mm/min. Load-displacement curves for tensile samples with the carbon fibre lamina at 0° (parallel to the load direction) are shown in Figure 10, whereas the curves for the case with the fibre direction at 90° (perpendicular to the load direction) are shown in Figure 11. Eight samples were tested for each bimaterial configuration, four samples with a notch and four samples without a notch. The load-displacement curves shown in Figures 10 and 11 were obtained directly using the displacement information from the grips, without using an extensometer.

The tensile strength, calculated as the failure load divided by the cross-sectional area of the sample, was evaluated. Both in the straight samples (without a notch) and in the modified samples (with a notch), the cross-sectional area was taken as the nominal one (thickness \times width) from the un-notched section. Table 1 shows the summary of tensile test results.

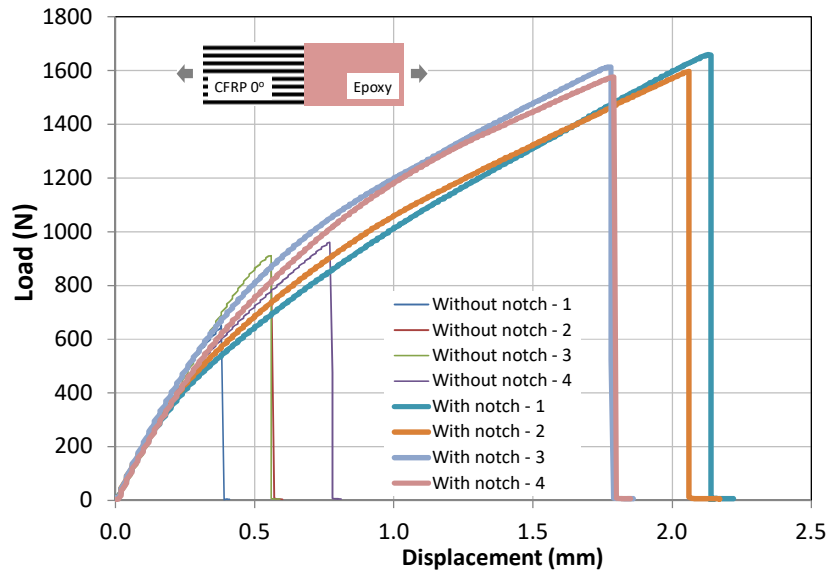


Figure 10. Tensile tests for samples with the carbon fibre at 0°.

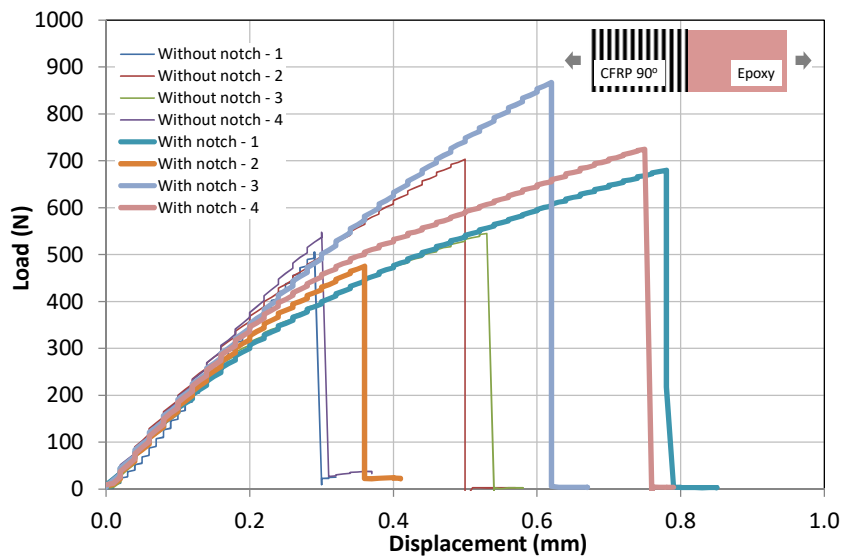


Figure 11. Tensile tests for samples with the carbon fibre at 90°.

Sample	Tensile strength (MPa)				Mean (MPa)	Std. Dev. (MPa)	CV (%)
	1	2	3	4			
0° without notch	11.6	16.6	17.8	18.0	16.0	3.0	18.7
0° with notch	31.7	30.5	30.8	30.2	30.8	0.7	2.1

90° without notch	9.1	12.7	9.8	10.0	10.4	1.6	15.2
90° with notch	12.3	8.5	16.3	13.6	12.7 ⁽¹⁾	3.3	25.7

⁽¹⁾ Mean value removing test “With notch – 2” is 14.1 MPa.

Table 1: Summary of tensile test results.

The tensile test results in Table 1 show that the presence of the notch on the epoxy (adhesive) part has a clear influence on the failure load. In the samples with the carbon fibre at 0° (associated with the failure path “b”), the presence of the notch increases the mean tensile strength value by 92% (in fact, the failure in the notched specimens does not occur just at the interface, but a little way into the epoxy side as well), whereas in the case of the carbon fibre at 90° (associated with failure path “c”), the tensile strength increase is 22% when all the results are considered. This increase is greater (35%), if the test result corresponding to sample “With notch – 2” is not taken into account, as this shows very different failure behaviour when compared to the other notched samples (see Figure 11). An explanation for the higher sensitivity to the notch elimination in the 0° configuration may be associated with the higher value of the order of stress singularity of the 0° configuration ($\lambda=0.219697$), compared to the 90° configuration ($\lambda=0.100345$), both for the un-notched case, i.e. $\alpha=90^\circ$ (see Figure 3).

3.3 Shear tests

Shear samples were tested using the Iosipescu device. Figures 12 and 13 show the load-displacement curves for the samples with the carbon fibres at 0° and 90°, respectively. Similarly, as in the case of the tensile tests, eight samples were tested (4 without the notch and 4 with the notch). The nominal shear strength was calculated by dividing the

failure load by the nominal cross-sectional area of the samples at the reduced neck section of the Iosipescu samples, where the bimaterial interface is located. Table 2 shows the summary of the shear test results.

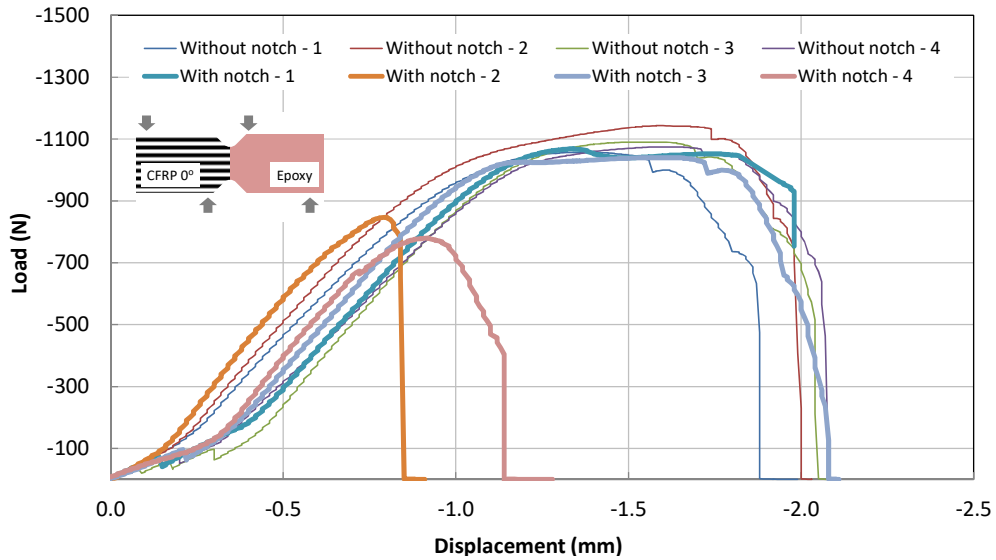


Figure 12: Shear (Iosipescu) tests for samples with the carbon fibre at 0° .

In the shear tests, in both test configurations (with the fibres at 0° and 90°), there is no clear influence of the presence of the notch on the failure load. The apparent difference in behaviour, mainly in displacements at the beginning of the tests (see Figure 13), between samples with the notch and samples without the notch, was found to be a small clearance of the jigs, which was corrected later. The presence of this clearance does not affect the failure load of the samples.

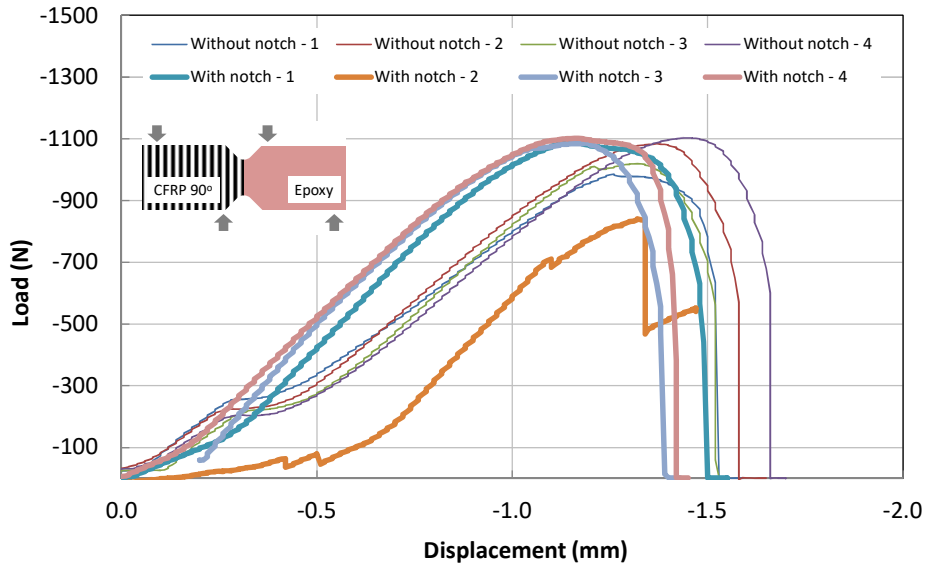


Figure 13: Shear (Iosipescu) tests for samples with the carbon fibre at 90°.

Sample	Shear strength (MPa)				Mean (MPa)	Std. Dev. (MPa)	CV (%)
	1	2	3	4			
0° without notch	31.9	33.3	32.2	32.4	32.5	0.59	1.8
0° with notch	31.7	24.9	31.2	23.4	27.8 ⁽¹⁾	4.28	15.4
90° without notch	28.0	30.4	28.6	30.6	29.4	1.3	4.4
90° with notch	31.1	23.9	30.3	30.6	30.7 ⁽²⁾	0.4	1.3

⁽¹⁾ Mean calculated removing samples “With notch – 2” and “With notch – 4” is 31.4 MPa.

⁽²⁾ Mean calculated removing sample “With notch – 2” which failed outside the interface.

Table 2: Summary of shear (Iosipescu) test results.

In the 0° configuration, samples with notch 2 and 4 should be discarded from the statistics as the failure in one of these cases was outside the interface, and in the other case, the sample presented some damage near the notch which gave rise to a premature failure. In the 90° configuration, the sample with notch 2 failed outside the interface as well and should not be taken into account for the calculations. These samples show, in Figures 12 and 13, a completely different behaviour from the rest of tests.

In the shear tests with the carbon fibre at 0° , even after eliminating samples 2 and 4 (with notch), which failed at a lower load than samples 1 and 3, the mean shear strength does not change significantly (32.5 MPa without notch, and 31.4 MPa with notch).

Something similar occurs with the shear tests where the carbon fibre is oriented at 90° , where only a slight increase in the shear strength appears, which is probably associated more with the dispersion of the experimental tests than with a clear influence of the notch over the failure.

4 Concluding remarks

The original idea by Lauke and Barroso [1] to evaluate the tensile strength of bimaterial joints was extended to anisotropic bi-materials and shear tests (Iosipescu) in order to evaluate the apparent adhesive shear strength of bimaterial joints with composite materials. In the present study, and in the framework of failure prediction of adhesive joints with composite materials, the tensile and shear strengths of bimaterial joints were obtained.

The free-edge stress singularities typically appearing in bimaterial samples were removed by adequate machining of the local configuration of the corner, creating a small notch at the interface on the adhesive side. The correct angle of this little notch was determined using a semi-analytical procedure to calculate the stress singularities and looking for the range of notch angles where the stresses become regular (bounded). Then, the samples were manufactured accordingly. FEM models were performed in order to confirm the disappearance of the stress singularities.

Tensile test results demonstrated the strong influence of the notch on the failure load and consequently, on the measured tensile strength value, almost multiplying by two the tensile strength in the case of the carbon fibre oriented parallel to the load direction (0°).

In contrast, shear (Iosipescu) tests did not show any clear influence of the notch over the shear strength, as the failure load was not altered in a demonstrable way.

A possible reason for this difference between the tensile and shear test results could be the difference in the interface area affected, or influenced, by the stress singularities. In the tensile test, most of the cross-sectional area of the sample is affected by the presence of the singularity stress field, and the whole perimeter of the interface needs to be machined with notches. By contrast, in the shear tests, only the edges along the thickness side are affected by the shear stress singularities and need to be machined. An additional explanation for the observed difference between the tensile and shear specimens is that in shear tests the interface zone close to the short free edge is more prone to plasticity effects in shear than in tension (thinking initially about the von Misses plasticity criterion, for example).

Previous works, already referenced, have also shown this strength increment in the tensile configuration when eliminating the stress singularity configuration [1,11].

Nevertheless, the important strength increment of a 92% was not referenced previously. This significant increment might be associated to the stiffness mismatch, higher than for isotropic material configurations, due to the presence of the unidirectional carbon fibre laminate.

In the case of shear stresses, Chowdhuri and Xia [8] tested isotropic bimaterial configurations in shear but using cylindrical samples in torsion. This gives rise only to shear stresses along the interface but with a non-uniform distribution, no shear strength values being reported for the non-singularity configuration to be compared with.

It can be concluded that, for the bimaterial configuration under analysis, a correct tensile strength determination in bimaterial composite joints requires the presence of the

notch (whose angle value depends on the local corner configuration), whereas for the shear strength determination, the presence of the stress singularity has not been shown to influence the failure load value.

Acknowledgements

The authors acknowledge the help of the students Pedro E. Romero and Alberto Martín in manufacturing the samples, and Antonio Cañas (Seville) and Dietmar Krause (Dresden) for the careful machining of the samples. The study was supported by the Junta de Andalucía and European Social Fund (Projects of Excellence, TEP-4051, TEP-4071), the Spanish Ministry of Economy and Competitiveness and European Regional Development Fund (Project MAT2012-37387).

References

- [1] Lauke B, Barroso A. Notched-butt test for the determination of adhesion strength at bimaterial interfaces. *Compos. Interface*. 2011;18:661-669.
- [2] Barroso A, Mantič V, París F. Representativity of the singular stress state in the failure of adhesively bonded joints between metals and composites. *Compos. Sci. Technol*. 2009;69:1746-1755.
- [3] Lauke B. Doubly-curved interfaces for adhesion strength testing. *Compos. Interface*. 2011;18:121–133.
- [4] Lauke B, Schüller T, Schneider K. Determination of interface strength between two polymer materials by a new curved interface tensile test. *Compos. Interface*. 2003;10:1–15.

- [5] Schneider K, Lauke B, Schüller T. Determination of the interface strength between two polymer materials by a new curved interface tensile test: preliminary experimental results. *Compos. Interface*. 2003;10:581–591.
- [6] Lauke B. Stress concentration along curved interfaces as basis for adhesion tests. *Compos. Interface*. 2007;14:307–320.
- [7] Wetherhold C, Dargush G.F. Improvement of adhesive strength at a bi-material interface by adjusting the interface angles at the free edge. *Theor. Appl. Fract. Mec*. 2015;77:69-73.
- [8] Chowdhuri MAK, Xia Z. An innovative method to determine bonding strength envelope based on theory of bi-material interface mechanics. *Procedia Engineering* 2011;10:118-123.
- [9] Wu Z. Stress concentration analyses of bi-material bonded joints without in-plane stress singularities. *Int. J. Mech. Sci*. 2008;50:641-648.
- [10] Bijak-Zochowski M, Waas AM, Anderson WJ, Miniatt CE. Reduction of contact stress by use of relief notches. *Exp Mech* 1991;31:271-275.
- [11] Wang P, Xu LR. Convex interfacial joints with least stress singularities in dissimilar materials. *Mech. Mater*. 2006;38:1001-1011.
- [12] Barroso A, Mantič V, París F. Singularity analysis of anisotropic multimaterial corners. *Int. J. Fracture*. 2003;119:1-23.
- [13] Mantič V, Barroso A, París F. Singular elastic solutions in anisotropic multimaterial corners. In: *Mathematical methods and models in composites*, V. Mantič (Ed.), Imperial College Press, 2014.

- [14] Shaw WT. *Complex Analysis with Mathematica*, Cambridge University Press, 2006, Cambridge.
- [15] Ting TCT. *Anisotropic Elasticity: Theory and Applications*. Oxford University Press, 1996.
- [16] Mantič V, París F, Berger J. Singularities in 2D anisotropic potential problems in multimaterial corners: Real variable approach. *Int. J. Solids Struct.* 2003;40:5197-5218.
- [17] Whitney JM. Effect of load distribution and placement in the Iosipescu shear test. *J. Reinf. Plast. Comp.* 1998;17:26-38.